Any immersion remote refocus (AIRR) microscopy

This project is maintained by amsikking in the York lab, and was funded by Calico Life Sciences LLC

Research article

Note that this is a limited PDF or print version; animated and interactive figures are disabled. For the full version of this article, please visit one of the following links: https://amsikking.github.io/any_immersion_remote_refocus_microscopy

Any immersion remote refocus (AIRR) microscopy

Alfred Millett-Sikking[1*]

[1]*Calico Life Sciences LLC, South San Francisco, CA 94080, USA*

[*] *Institutional email: amsikking+AIRR@calicolabs.com ; Permanent email: amsikking+AIRR@gmail.com*

Group website: andrewgyork.github.io

Abstract

3D imaging is essential for studying many biological processes. In microscopy we often collect volumes using standard focus to take a series of 2D images. For standard focus we avoid aberrations by matching the refractive index (RI) of the sample to the immersion of the objective, an awkward constraint for microscope users and designers. We can also focus with remote refocus (RR) optics, but these are traditionally restricted to the immersion of the objective, leaving little flexibility in choosing the sample RI. Here we present a versatile approach to aberration-free 3D imaging, where an objective of any immersion can be combined with a sample of any RI. For example, we can look into a watery sample with a Nikon 40x0.95 air objective, and use RR optics to extend the focal range from ~6μm to ~151μm. Avoiding liquid immersion is convenient for users and great for automated microscopy. Similarly, we can extend the range of a Nikon 40x1.30 oil objective from ~8μm to ~65μm

in water, and enjoy a larger field of view and numerical aperture (NA) compared to the equivalent water immersion objective. We can apply this method to use different objectives on the same system, with immersion-free, maximum depth and maximum NA modalities. In addition, we present a dynamic zoom lens to enable fast RR tuning in the RI range 1.33-1.51, which maximizes performance for a diverse range of biological samples. By combining different objectives with dynamic RR optics we can make an 'any' immersion microscope with a boosted focal range.

Intended audience

Microscope users, builders and developers.

Peer review status

First published _blank_ (This article is not yet peer-reviewed)

Cite as: _blank_

Introduction

Imaging samples in 3D with high spatial resolution is essential for studying many biological processes. In microscopy, we typically collect 2D images with an objective lens near the sample, and high spatial resolution is mostly achieved with high numerical aperture (NA). To get 3D data we routinely take a series of 2D images at different depths, or focal planes, and use these images to construct a volume we can explore.

Here we discuss the mechanisms and limitations of two different focus methods we refer to as "standard focus" and "remote refocus" (RR). We then show how these methods can be combined to produce a microscope with a boosted focal range for any combination of immersion medium and sample refractive index (RI). The design options we explore here are readily applied to systems with existing RR optics, like single-objective light-sheet (SOLS) microscopes.

Standard focus

To change the focal plane on a typical widefield microscope we usually move the objective towards the sample, a method we refer to here as "standard focus". The maximum range of this operation is mechanically limited by the distance between the front of the objective and the image plane, usually called the working distance (WD). However, the range of standard focus may be dramatically reduced by the choice of sample RI, which is an awkward reality for microscope users and designers. To understand (and avoid) this effect we can consider the focusing process in more detail.

We can think of the space between the front of the objective and the image plane as the 'final elements' in the lens design, where the shape and RI matter (especially at high NA). The shape is fixed by the image plane and the final solid surface of the objective (usually a glass lens). The RI is set by the intended *immersion* medium for

the objective, for example air, water or oil (and sometimes a coverslip). Deviating from the intended shape or RI can produce severe aberrations and blurry images.

When we use standard focus to image deeper into a sample, layers or 'slabs' of intended immersion (like air, water or oil) are effectively exchanged for slabs of sample. If we *match* the sample RI to the immersion, then this is a null operation and the objective will image as designed (Figure 1, 1/3). However, if we have some RI *mismatch*, then the slab of sample (with unintended RI) will produce spherical aberration, and make the images blurry with enough depth (Figure 1, 2/3 and 3/3) [Pawley 2006]. **So, for standard focus we must match the sample refractive index to the immersion to avoid aberrations**:

$$n_i = n_s \tag{1}$$

where n_i and n_s are the immersion and sample RI respectively.

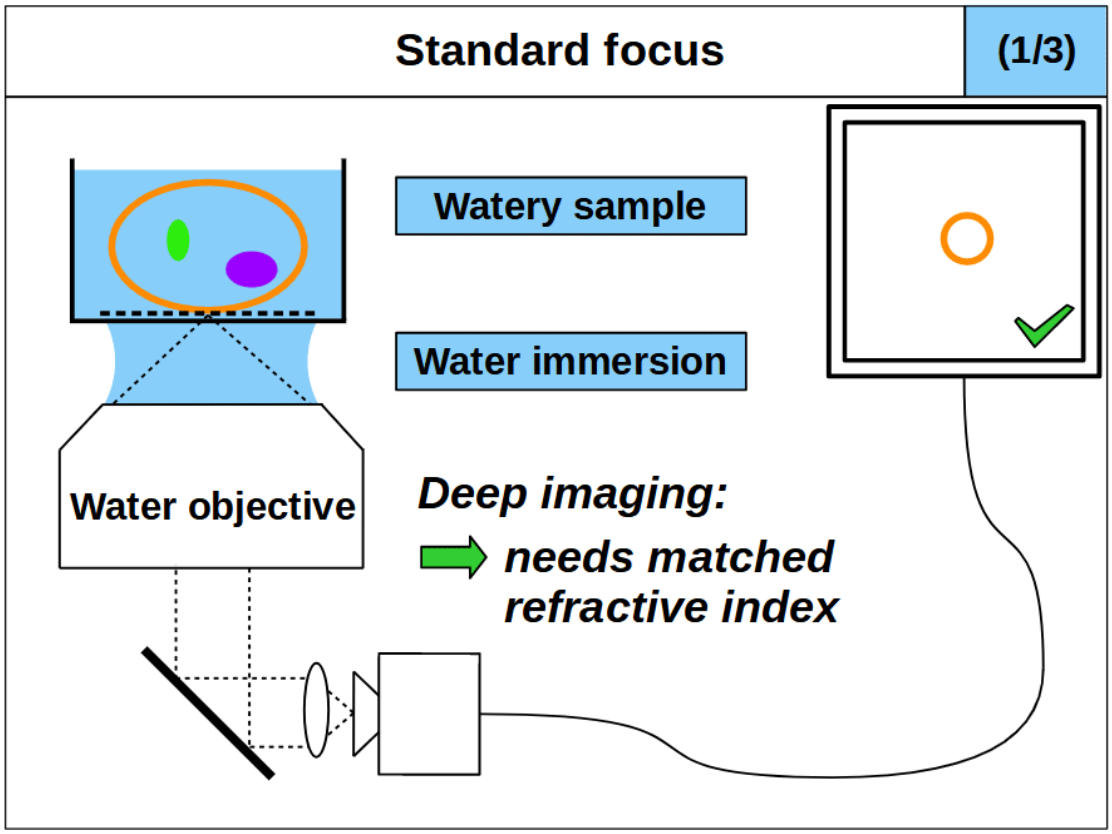

Figure 1: Standard focus into a watery sample with water, air and oil immersion. This cartoon shows a watery 3D sample (like a cell in media) being imaged at different depths by a standard widefield microscope (objective + tube lens). The image is formed at the camera and relayed to the cartoon screen, which shows image planes at different depths in the sample as the objective moves up and down. **Animation 1/3** shows a water immersion objective that is refractive index *matched* to the sample, giving good images at depth. **Animation 2/3** shows an air objective that is refractive index *mismatched* to the sample and therefore gives blurry imaging from depth induced spherical aberration. **Animation 3/3** shows an oil immersion objective that (like animation 2/3) is also refractive index *mismatched* giving blurry images with depth.

Our need to refractive index match the sample to the immersion for 3D imaging is awkward. The RI of biological samples varies significantly, leaving microscope users and designers chasing around between different immersion options (with no flexible solution). Air immersion is the most convenient and is excellent for high-speed tiling, but it has the lowest NA and low depth penetration due to the large RI difference. Water immersion is usually a good RI match for live samples, but it requires regular hydration (from evaporation) and has the lowest NA of the liquid immersions. Oil immersion offers the highest NA, and is insensitive to coverslip thickness, but struggles with depth from the RI mismatch. A good compromise between NA and RI matching is silicone oil immersion, but this is still cumbersome in tiling applications.

Remote refocus

As an alternative to standard focus, remote refocus (RR) optics [Botcherby 2007] can also be used to image different focal planes in the sample. RR has become an important foundation in high-speed 3D imaging applications [Millett-Sikking 2018], most notably in the recent uptake of single-objective light-sheet (SOLS) microscopes [Millett-Sikking 2019, E. Sapoznik 2020, Chang 2021, Yang 2022, Chen 2022].

The main feature of an RR setup is the ability to adjust the focal plane without moving the primary objective or the sample, for example by moving one of the downstream objectives (Figure 2, 1/3). In contrast to standard focus, where the RI of the immersion and the sample must match, in RR we can exchange slabs of *different* RI between the sample and the remote volume. For example, it is common to use air immersion in the remote space with an aqueous sample. We avoid spherical aberration by setting the magnification between the sample and remote space M_{RR} to preserve angles:

$$M_{RR} = \frac{n_s}{n_{RR}} \tag{2}$$

where n_{RR} is the immersion of the remote space.

It is traditional to *assume* that the sample RI matches the immersion, and to configure the RR optics for this RI. However, in the case where the sample RI and immersion are not matched, **we should optimize the remote refocus for the refractive index of the sample, not the immersion of the objective.**

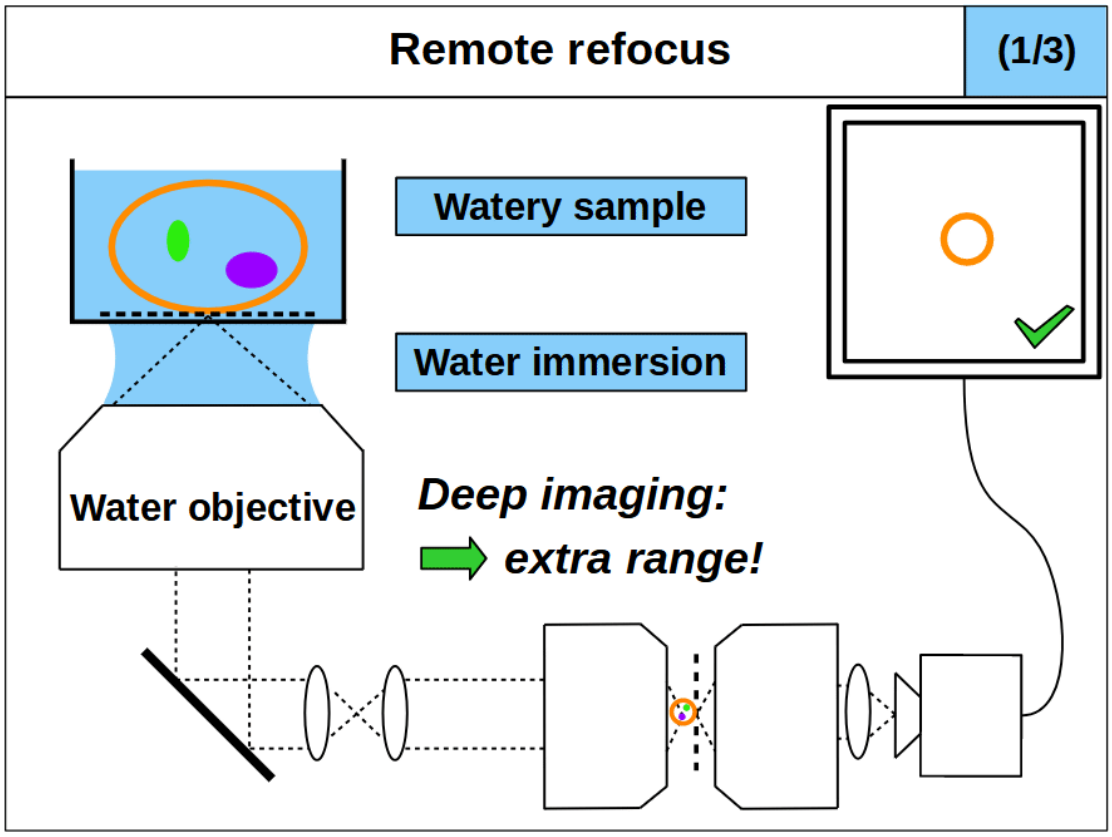

Figure 2: Remote refocus into a watery sample with water, air and oil immersion. This cartoon shows a watery 3D sample (like a cell in media) being imaged at different depths by a remote refocus (RR) microscope (a widefield microscope + 2 additional microscopes). The optics in the first 2 microscopes (widefield microscope + tube lens + objective) are configured to produce an aberration-free 3D copy of the sample in the remote space, which is then re-imaged by the 3rd microscope (objective + tube lens). **Note: the RR optics are set for a watery sample, regardless of the immersion used by the primary objective.** The final image is formed at the camera and relayed to the cartoon screen, which shows image planes at different depths in the sample as the objective in the 3rd microscope moves back and forth. **Animation 1/3** shows a water immersion objective that is refractive index *matched* to the sample. In this configuration the standard focus and RR both have maximum range, although only the RR range is animated here (giving extra range over standard focus). **Animation 2/3** shows an air objective that is refractive index *mismatched* to the sample, greatly reducing the range of standard focus. However, the RR is still optimized for a watery sample, and so the remote range persists. **Deeper immersion-free microscopy** is available in this configuration. **Animation 3/3** shows an oil immersion objective that (like animation 2/3) is also refractive index *mismatched* (reducing the range of standard focus). However, like animation 2/3, the RR is still optimized for a watery sample and the range persists. **Deeper maximum NA microscopy** is available in this configuration.

Using standard focus and remote refocus together

In a typical RR microscope we would match the sample RI with the immersion for standard focus (equation 1), and we would configure the RR optics for the sample (equation 2), yielding maximum range for both focus methods. However, a key realization is that if the RI of the sample and immersion differ, then the range of

standard focus will reduce, but the RR range persists. Conversely, if we match the sample RI with the immersion, but the RR is optimized for a different RI, then the RR range will reduce and the standard focus range will persist. **So we can choose to optimize standard focus and remote refocus for different refractive indices, which reveals new design options.**.

It is counter intuitive to deviate from the 'usual' system design, where we match the immersion and RR optics for the same RI. However, there are some compelling options:

- **Deeper immersion-free microscopy:** we can combine a high NA air objective (with very limited standard focus range in liquids) with a remote refocus optimized for liquid (Figure 2, 2/3). Avoiding liquid immersion is very convenient for users and great for automated microscopy, like time-lapse imaging or high-speed tiling.
- **Deeper maximum NA microscopy:** we can combine a high NA oil objective (with reduced standard focus range in watery samples) with a remote refocus optimized for water (Figure 2, 3/3). Oil immersion is coverslip insensitive and offers the maximum NA for live biological samples, exceeding that of high quality water immersion objectives.
- **Any sample refractive index microscopy:** by decoupling the choice of immersion from how we configure the RR, we can set the RR optics (via equation 2) to image deeper into any sample. For example, we can continuously tune the RR for any sample RI in the range 1.33-1.51 and access aberration-free volumes that have traditionally been unavailable (Figure 5).
- **Any immersion microscopy:** by combing different objectives with tunable RR optics we can get aberration-free volumes with any immersion and any sample RI on the same microscope. So we can have single instrument with with immersion-free, maximum depth and maximum NA modalities.

We gear the rest of this article towards exploring new design options for high NA 3D microscopy, although we note that these findings are not limited to this regime, and compelling applications may be found with lower NA and larger field of view systems. In the results section we compare standard focus to RR for some attractive choices of primary objective, and show a concrete example of tunable RR optics. In the data section we demonstrate the power of the technique by imaging deep into a watery sample with a high NA air objective (that would normally give very blurry images). For the discussion section we consider an attractive microscope design and review the main benefits of the technology.

Results

To evaluate the deeper imaging potential of a remote refocus microscope (Figure 2) compared to a widefield setup (Figure 1), we take a practical approach and model how a series of commercially available objectives compare in each configuration. For the sake of simplicity, we limit our search to a collection of Nikon objectives that are compatible with SOLS microscope design (a compelling use case for RR optics). We can therefore constrain the numerical aperture, focal length and immersion medium for a given setup, although we point out that these ideas can be applied to other manufacturers, and at lower NA. We can then calculate the standard focus and remote refocus ranges as a function of the sample refractive index n_s over the biological range:

$$1.33 \leq n_s \leq 1.51 \tag{3}$$

Standard focus range

In Figure 3 we compare the accessible imaging range of different objectives in a widefield microscope. In particular we plot the diffraction limited depth of standard focus as a function of the sample RI according to equation a8. The interactive figure can be toggled between linear and log scales for the highest NA objectives, and those with the 'most pixels' (N_{px}). For example, in the high NA category, the 100x1.35 silicone oil objective offers the best compromise for varying sample types, with a minimum range of 10µm for any RI. However, if the samples are mostly aqueous, then the 60x1.27 water lens has a much larger range (limited by the working distance at 180µm). The 40x0.95 air objective is perhaps the worst option for depth, offering only ~6µm for any liquid sample (visible on the log scale). The 100x1.45 oil may be the least attractive option for live biology, with the inconvenience of liquid immersion and the lowest range in watery samples (forcing the 3µm lower bound). Similar trends can be seen in the most pixels category.

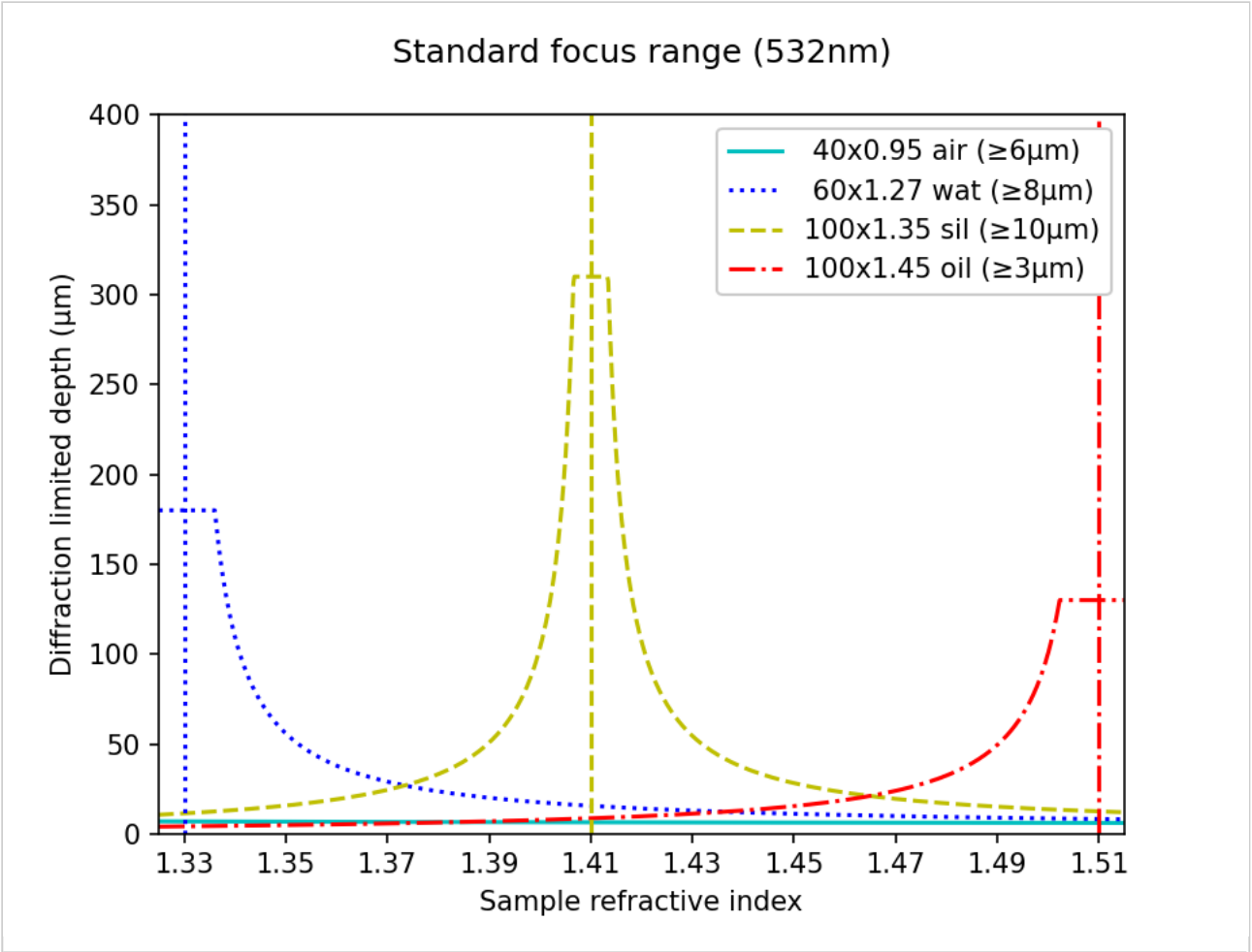

Nikon objectives: Highest NA Depth scale: linear

Figure 3: the standard focus range of a widefield microscope. The diffraction limited imaging depth is plotted as a function of sample refractive index for a collection of Nikon objectives at 532nm (equation a8). The figure is interactive and can be toggled between linear and log scales for objectives with the highest NA and those with the most pixels. The curves are truncated at the working distance of each objective and vertical reference lines are added for the standard immersions (water=1.33, silicone=1.41 and oil=1.51).

Standard focus with remote refocus range

In Figure 4 we present the combined range of a widefield microscope with RR optics according to equation a11. In this setup, the primary objectives are still limited to a particular immersion, but we can (in principle) tune the RR optics continuously across the range of the sample RI (shown here). All of the configurations now benefit from the extra range provided by the RR. In particular, in the high NA category the lower bound on the 100x1.45 oil lens has now jumped from 3µm to 35µm, converting it into an attractive option for many applications. In practice, this delivers deeper imaging at **maximum NA** for any sample RI under 1.45. Most apparent in the high NA category is the large increase in depth now available to the 40x0.95 air objective, offering deeper **immersion-free** imaging up to 151µm!

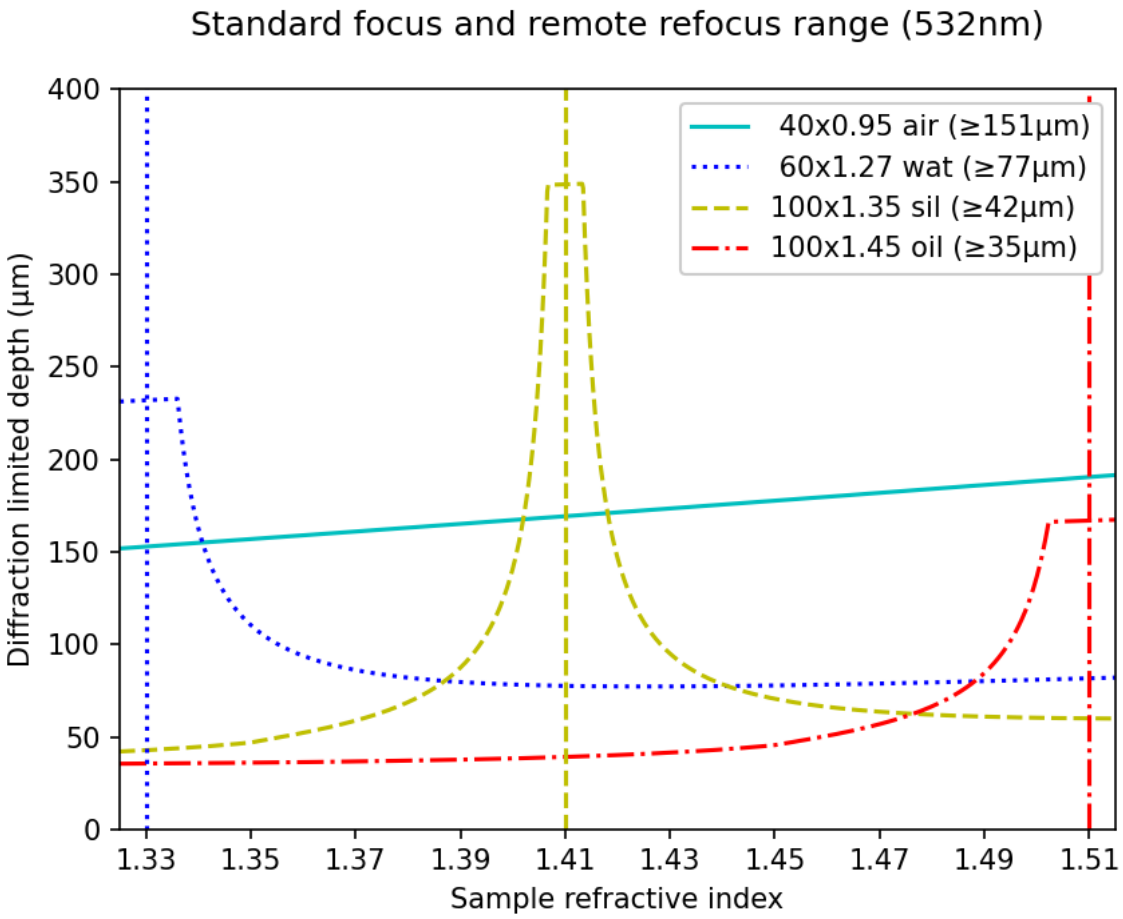

Nikon objectives: Highest NA ▾ Depth scale: linear ▾

Figure 4: the combined range of a widefield microscope with remote refocus optics. The diffraction limited imaging depth is plotted as a function of sample refractive index for a collection of Nikon objectives at 532nm (equation a11). The figure is interactive and can be toggled between linear and log scales for objectives with the highest NA and those with the most pixels. The curves are truncated at the working distance of each objective and vertical reference lines are added for the standard immersions (water=1.33, silicone=1.41 and oil=1.51).

Dynamic remote refocus

In the introduction, we discuss how the RR magnification should be set according to equation 2, and that we should optimize for the sample RI (not the immersion). Previously, we used static optical configurations to set the RR magnification for a particular immersion [Millett-Sikking 2019], with the hope that the sample would not deviate much from this RI.

Here we present a dynamic zoom lens to enable fast RR tuning in the refractive index range 1.33-1.51, which maximizes performance for a diverse range of biological samples (Figure 5). Our design uses inexpensive stock parts, maintains constant track length and telecentricity, and is diffraction limited across the visible spectrum and standard sCMOS field of view (see appendix for details). Specifically this module is intended to replace the tube lens in the second microscope of an RR system, and provides a concrete design to enable the focal ranges shown in Figure 4.

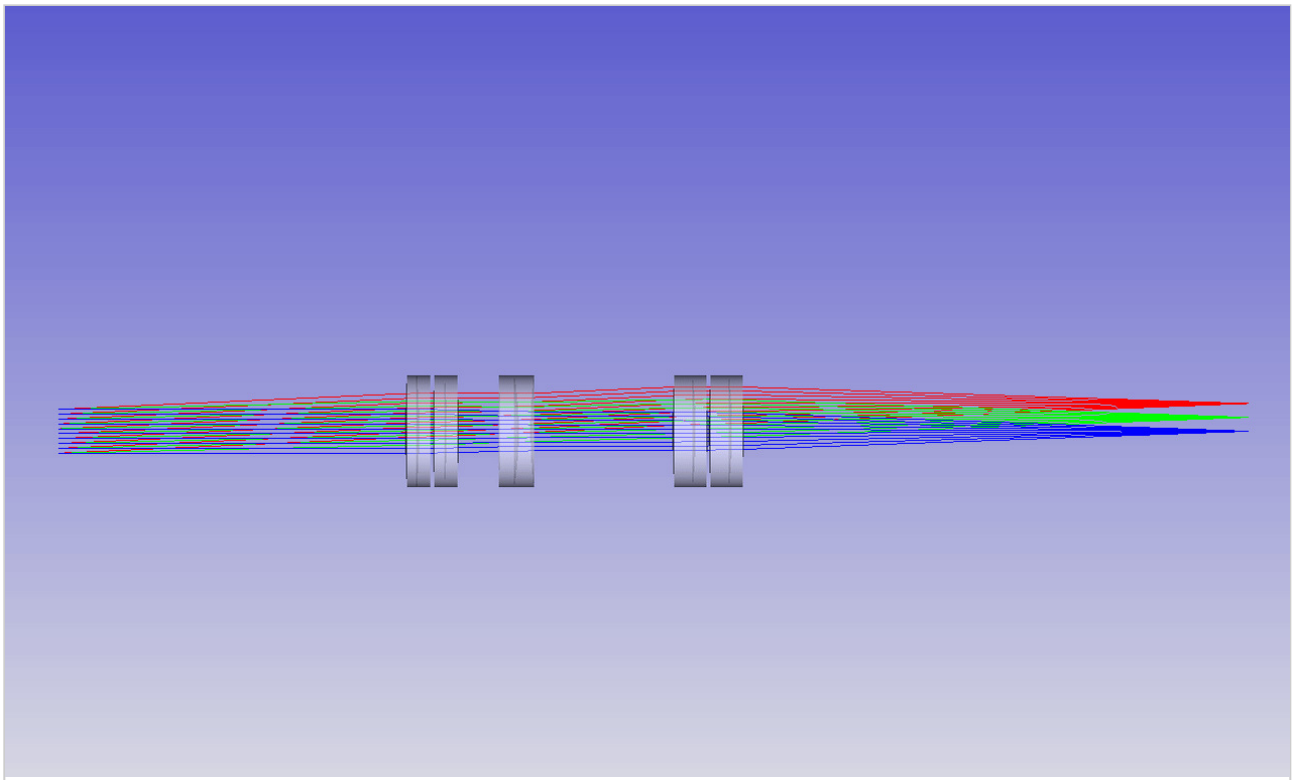

Figure 5: Dynamic zoom tube lens. This animation shows an example of a zoom lens that can replace a static tube lens in a remote refocus microscope. In this version the focal length varies continuously as the elements are moved, allowing the magnification of the RR to be tuned across the biological refractive index range 1.33-1.51. The lens uses inexpensive stock parts, maintains constant track length and telecentricity, and is diffraction limited across the visible spectrum and standard sCMOS field of view (see appendix for details).

Data

To demonstrate the power of the 'any immersion' concept we built a prototype large field of view SOLS microscope with (static) RR optics tuned for water (see here for instrument details). We then used this platform to directly **compare a Nikon 40x1.15 water objective against a Nikon 40x0.95 air objective imaging deep into a watery sample** (fluorescent beads in agarose). We picked this example since the RI mismatch between

air and water is very high, and so the benefit of the RR range compared to the standard focus range is particularly pronounced.

Water objective

We use the 40x1.15 water objective as the 'benchmark' for a typical optical configuration, where the immersion and sample have the same RI. In this mode the volumetric point spread function (PSF) is insensitive to standard focus, so we can move the primary objective up and down to access different depths (Figure 6). The main benefits of this setup are an increased NA and total focus range (standard + RR), in exchange for the inconvenience of the water immersion.

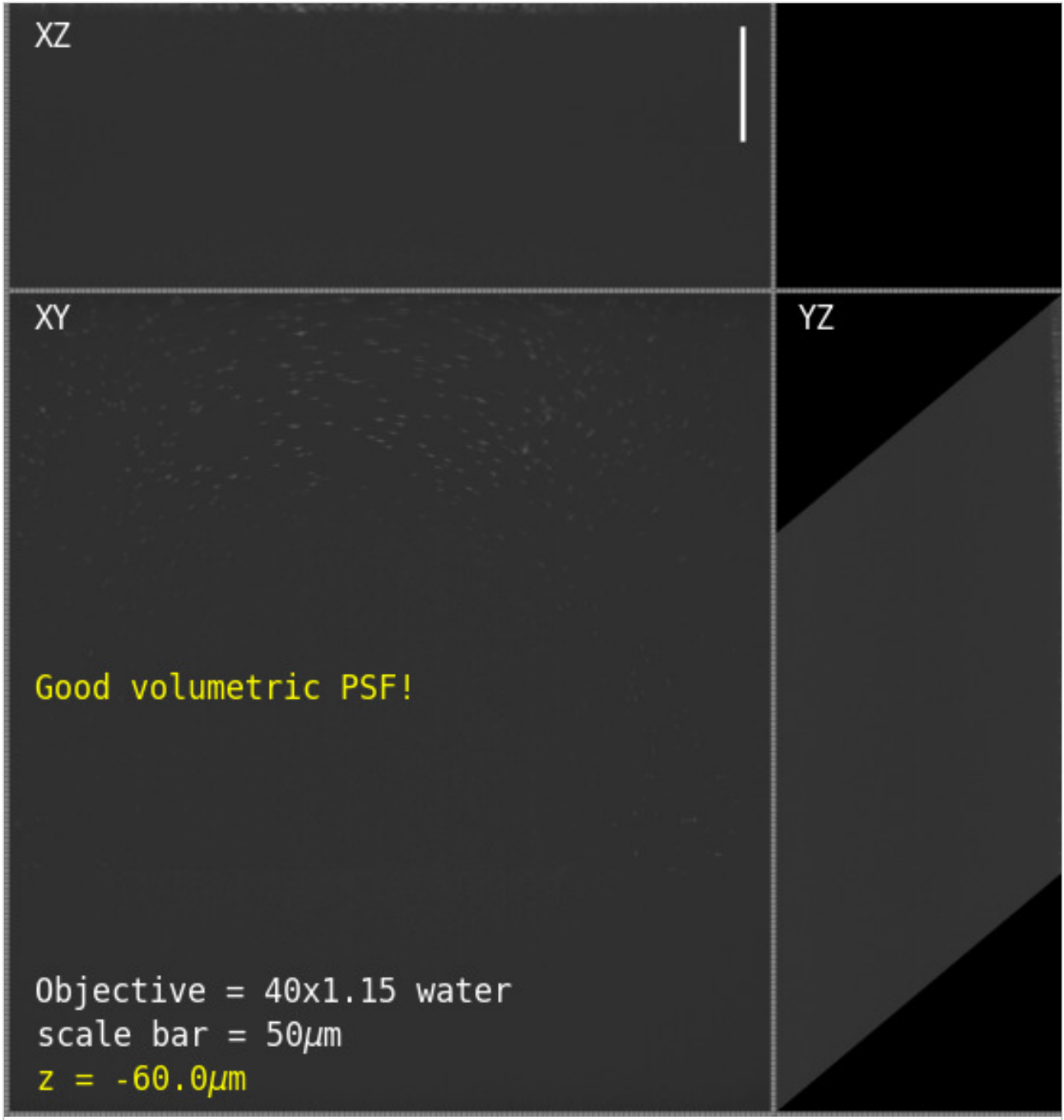

Figure 6: PSF vs standard focus for a 40x1.15 water objective. This animation shows the volumetric point spread function of a Nikon 40x1.15 water immersion objective as a function of standard focus (z). The

fluorescent beads were prepared in a watery gel according to this protocol. Since the sample RI *matches* the water immersion the PSF is insensitive to standard focus, allowing an increased range of focus (standard + remote) when using the microscope in this modality. **Note:** each frame of the animation shows the max projections of the entire volume (~330x355x125)μm^3 in traditional XY, XZ and YZ coordinates.

Air objective

We can now *swap* the 40x1.15 water objective for the 40x0.95 air objective on the same microscope and get good volumetric PSF deep into the watery gel! Normally the depth of standard focus is limited to about ~6µm (Figure 3), but here we can clearly image > 50µm (Figure 7). This mode has the benefit of being immersion-free, with the drawback of slightly lower NA and a greatly reduced standard focus range.

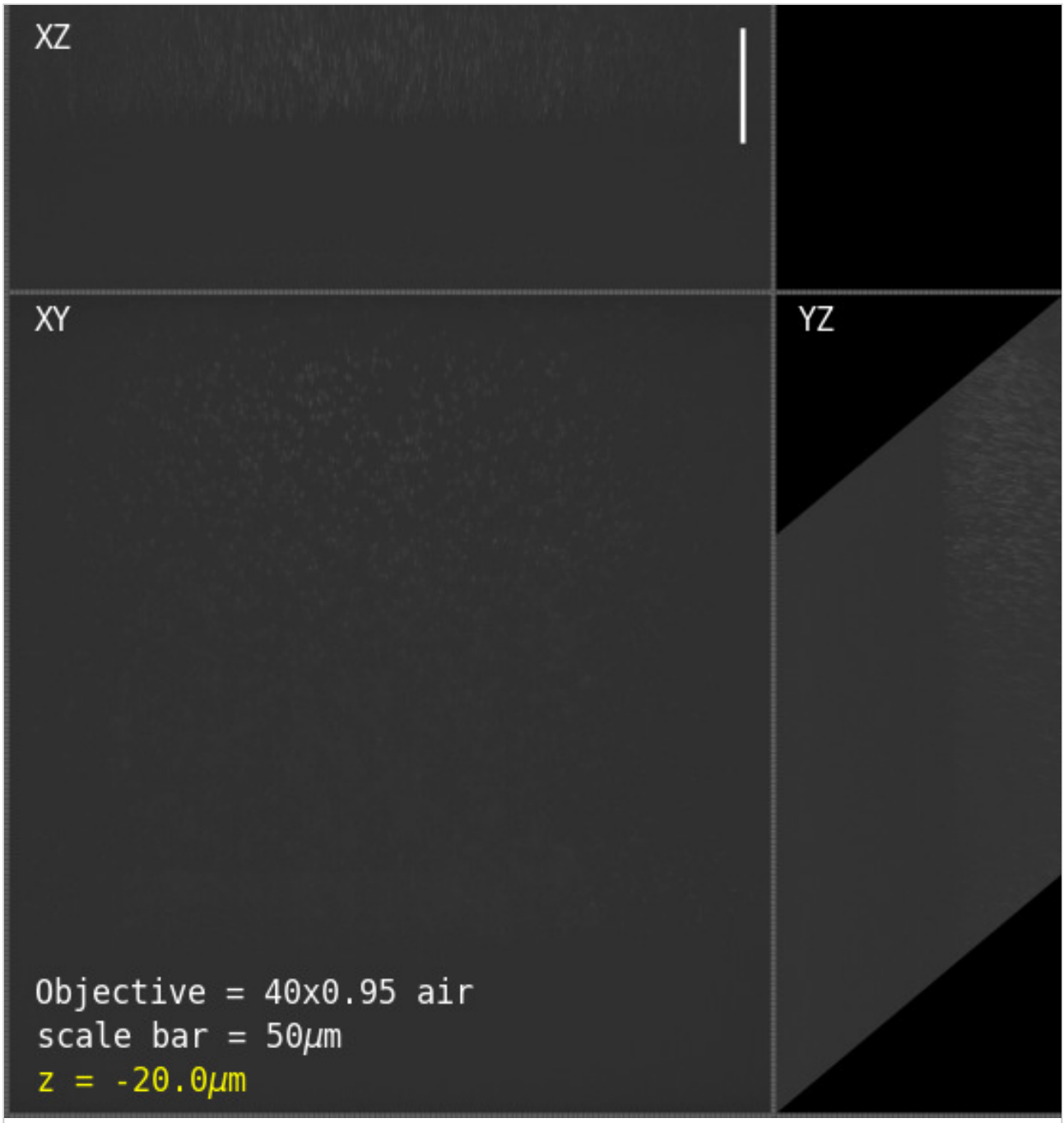

Figure 7: PSF vs standard focus for a 40x0.95 air objective. This animation shows the volumetric point spread function of a Nikon 40x0.95 air objective as a function of standard focus. The fluorescent beads were prepared in a watery gel according to this protocol. Since the sample RI strongly *mismatches* the air immersion the PSF is highly sensitive to standard focus. However, as predicted by the results section, there is a ~6μm range over which the remote refocus volume is good, allowing deeper immersion-free imaging when using the microscope in this modality (i.e. for convenience or high speed tiling etc). **Note:** each frame of the animation shows the max projections of the entire volume (~330x355x125)μm^3 in traditional XY, XZ and YZ coordinates.

Point spread function

If we 'park' the standard focus in a good place for both the water and air objectives (i.e. at 'zero' depth where the focal plane is just above the coverslip) then we can compare the PSF in both configurations over the volume (~330x195x65μm^3). For the **water objective PSF** we found full width half max (FWHM) values in the range **(425-582)nm radially and (1.38±0.11)μm axially** (2577 beads used for statistics). For the **air objective PSF** we found FWHM values in the range **(422-550)nm radially and (2.08±0.07)μm axially** (2716 beads). As expected the water objective has notably improved axial PSF due to the higher NA. The higher NA should also show in a reduced radial PSF but the current instrument prototype was originally optimized for the air objective so there is some vignetting at objective 2 and the pixel size (~220nm) is too large (addressed here with an improved design). Overall these PSF results are in line with similar microscopes like DaXi which gave (380-480)nm radial and (1.86±0.17)μm axial [Yang 2022] or tiling OPM with (390-430)nm radial and (1.22±0.13)μm axial [Chen 2022].

Discussion

In contrast to conventional microscopy, we have shown that we can use RR optics to collect aberration-free 3D volumes for any combination of immersion and sample RI. The method is quite general, and applies to high and low NA systems with many configuration options. To highlight some of the advantages of this new design space, we target the discussion towards high NA systems for *watery samples* that are most relevant to 3D time-lapse imaging (like living cells and organisms).

If we restrict the microscope to a widefield, then we can see that the 60x1.27 water objective has the highest diffraction limited depth for any sample RI under ~1.36 (Figure 3). In this regime the other objectives (air, silicone and oil) are best used for shallow 3D samples (< 10μm) or speciality situations where the lack of immersion or marginal increase in NA are required (like high-speed 2D tiling or TIRF microscopy). With a 333μm field of view, a theoretical resolving power of ~250nm and ~2600 pixels, the 60x water objective is a good match for current sCMOS cameras (specifications from table). Although water objectives are sensitive to coverslip tilt, thickness and require regular hydration, the 60x1.27 offers the best 3D imaging performance for watery samples in the high NA category.

If we now consider a remote refocus microscope (like a SOLS system), we can see a new series of configurations that significantly outcompete widefield in terms of volumetric range and NA (Figure 4). For example, we can combine an RR optimized for water with multiple objectives, like a 40x1.15 water objective for

maximum depth (600µm for MRD77410), a 40x0.95 air objective for **immersion-free** speed and convenience, and a 40x1.30 oil objective for **maximum NA**. Because these lenses have the same focal length they are *interchangeable* on the same system, and at 40x magnification, they offer larger fields of view (500µm) and pixel counts (> 2927) than the 60x1.27 water objective (the leading widefield option).

We propose that remote refocus optics should be configured for the sample RI, and not the immersion of the objective. We acknowledge that for the same or similar samples this may be achieved with static optical configurations. However, we present a dynamic zoom lens to quickly tune the RR optics for the biological refractive index range 1.33-1.51, which minimizes aberrations for a diverse range of samples. This has the additional benefit of avoiding the axial 'stretching' ($n_i > n_s$) and 'squashing' ($n_i < n_s$) distortions from focusing with mismatched immersion [Diel 2020]. **We propose that a dynamic magnification compensator is the preferred way to build a remote refocus microscope when imaging samples of varied refractive index.**

We find the **immersion-free** configurations particularly attractive for high throughput screening applications [Maioli 2016], where the benefit of high-speed tiling can greatly outweigh the slightly lower NA of an of air objective compared to liquid immersion options. In this regime, the increase in depth of a remote refocus microscope over a widefield is substantial, for example 151µm vs 6µm for the 40x0.95 air objective. We also find the thermal isolation from the 'air gap' appealing, avoiding the need to heat the objective for incubated samples. In addition, the stronger reflections from the air to coverslip boundary could be beneficial for hardware autofocus systems.

We see the coverslip insensitive oil immersion options with **maximum NA** as a great option for 3D super resolution [Zanacchi 2011] and low light experiments [Betzig 2006] that benefit from the highest angular collection at the primary objective. For example, the 40x1.30 oil objective from the 'most pixels' category can now be considered near maximum NA for water samples up to a diffraction limited depth of 65µm, making it an impressive option for many applications.

Given the 'mix and match' nature of the design space and the strong dependency on sample RI, we encourage builders to absorb the ideas presented here, run their own calculations, and then build the best system for their application. **This is a 'game changer' from the perspective of microscope users and designers, since we can now access aberration-free volumes over an extended range, for any combination of immersion or sample refractive index.**

Acknowledgements

This work was funded and supported by Calico Life Sciences LLC, and we would like to acknowledge the fantastic research environment that has been created here by the senior staff. We have enjoyed a spectacular level of freedom and support that has made this work possible.

In particular I acknowledge Andrew G. York for the uniquely innovative environment he has championed at Calico, and his ongoing scientific mentorship and support.

Appendix

Additional details can be found in the appendix.

References

1. [Pawley 2006] Handbook of Biological Confocal Microscopy, third edition; J. Pawley; Springer US, ISBN 978-0-387-25921-5, eBook ISBN 978-0-387-45524-2, (2006) https://doi.org/10.1007/978-0-387-45524-2
2. [Botcherby 2007] An optical technique for remote focusing in microscopy; E.J. Botcherby, R. Juškaitis, M.J. Booth and T. Wilson; Optics Communications, vol 281(4), p880-887, (2007) https://doi.org/10.1016/j.optcom.2007.10.007
3. [Millett-Sikking 2018] Remote refocus enables class-leading spatiotemporal resolution in 4D optical microscopy; A. Millett-Sikking, N.H. Thayer, A. Bohnert and A.G. York; (2018) https://doi.org/10.5281/zenodo.1146083
4. [Millett-Sikking 2019] High NA single-objective light-sheet; A. Millett-Sikking, K.M. Dean, R. Fiolka, A. Fardad, L. Whitehead and A.G. York; (2019) https://doi.org/10.5281/zenodo.3244420
5. [E. Sapoznik 2020] A versatile oblique plane microscope for large-scale and high-resolution imaging of subcellular dynamics; E. Sapoznik, B. Chang, J. Huh, R.J. Ju, E.V. Azarova, T. Pohlkamp, E.S. Welf, D. Broadbent, A.F. Carisey, S.J. Stehbens, K. Lee, A. Marín, A.B. Hanker, J.C. Schmidt, C.L. Arteaga, B. Yang, Y. Kobayashi, P.R. Tata, R. Kruithoff, K. Doubrovinski, D.P. Shepherd, A. Millett-Sikking, A.G. York, K.M. Dean and R.P. Fiolka; (2020) https://doi.org/10.7554/eLife.57681
6. [Chang 2021] Real-time multi-angle projection imaging of biological dynamics; B. Chang, J.D. Manton, E. Sapoznik, T. Pohlkamp, T.S. Terrones, E.S. Welf, V.S. Murali, P. Roudot, K. Hake, L. Whitehead, A.G. York, K.M. Dean and R.P. Fiolka; (2021) https://doi.org/10.1038/s41592-021-01175-7
7. [Yang 2022] DaXi—high-resolution, large imaging volume and multi-view single-objective light-sheet microscopy; B. Yang, M. Lange, A. Millett-Sikking, X. Zhao, J. Bragantini, S. VijayKumar, M. Kamb, R. Gómez-Sjöberg, A.C. Solak, W. Wang, H. Kobayashi, M.N. McCarroll, L.W. Whitehead, R.P. Fiolka, T.B. Kornberg, A.G. York and L.A. Royer; (2022) https://doi.org/10.1038/s41592-022-01417-2
8. [Chen 2022] Increasing the Field-of-View in Oblique Plane Microscopy via optical tiling; B. Chen, B. Chang, F. Zhou, S. Daetwyler, E. Sapoznik, G.M. Gihana, L.P. Castro, M.C. Sorrell, K.M. Dean, A. Millett-Sikking, A.G. York and R.P. Fiolka; (2022) https://doi.org/10.1364/BOE.467969
9. [Diel 2020] Tutorial: avoiding and correcting sample-induced spherical aberration artifacts in 3D fluorescence microscopy; E.E. Diel, J.W. Lichtman and D.S. Richardson; (2020) https://doi.org/10.1038/s41596-020-0360-2
10. [Maioli 2016] Time-lapse 3-D measurements of a glucose biosensor in multicellular spheroids by light sheet fluorescence microscopy in commercial 96-well plates; V. Maioli, G. Chennell, H. Sparks, T. Lana, S. Kumar, D. Carling, A. Sardini and C. Dunsby; (2016) https://doi.org/10.1038/srep37777
11. [Zanacchi 2011] Live-cell 3D super-resolution imaging in thick biological samples; F.C. Zanacchi, Z. Lavagnino, M.P. Donnorso, A.D. Bue, L. Furia, M. Faretta and A. Diaspro; (2011) https://doi.org/10.1038/nmeth.1744

12. [Betzig 2006] Imaging Intracellular Fluorescent Proteins at Nanometer Resolution; E. Betzig, G.H. Patterson, R. Sougrat, O.W. Lindwasser, S. Olenych, J.S. Bonifacino, M.W. Davidson, J. Lippincott-Schartz and H.F. Hess; (2006) https://doi.org/10.1126/science.1127344